Antiferromagnetic coupling in Fe/Cu/Fe and Co/Cu/Co multilayers on Cu(111)

W. F. Egelhoff Jr. and M. T. Kief
Surface and Microanalysis Science Division, National Institute of Standards and Technology, Gaithersburg, Maryland 20899
(Received 6 September 1991)

The magneto-optical Kerr effect has been used to investigate the exchange coupling between Fe and Co bilayers through Cu spacer layers. The films were grown on a Cu(111) substrate by molecular-beam-epitaxy (MBE) techniques under a variety of conditions, including both high vacuum and ultrahigh vacuum, substrate temperatures of 80, 300, and 500 K, and in the presence of as well as in the absence of electron bombardment. None of these films showed consistent evidence of antiferromagnetic (AFM) coupling, and there was no evidence of any consistent trends attributable to oscillatory AFM coupling. These results stand in marked contrast to results recently reported on similar multilayers that were grown by magnetron sputtering methods and that exhibit the giant magnetoresistance effect. These magnetron-grown multilayers, which are reported to be (111) textured, exhibit pronounced oscillatory AFM coupling. One possible resolution of these conflicting observations lies in the fact that oscillatory AFM coupling does occur in MBE-grown multilayers on Cu(100). Preliminary x-ray-diffraction pole-figure measurements on three of the magnetron-grown multilayers indicate that the tendency to (111) texture is not very strong, and that the multilayers contain crystalline grains other than (111). Thus, the AFM coupling that these multilayers exhibit could be at least partly a result of a minority constituent of crystalline grains oriented at or near (100). However, it cannot be proven that the near-(100) grains are entirely responsible for the AFM coupling in the magnetron-grown multilayers. Grains of other orientation may also contribute, but surprisingly, the present work implies that the (111)-oriented grains do not contribute.

I. INTRODUCTION

The giant magnetoresistance (GMR) effect in magnetic multilayers[1-3] has stimulated much interest in the antiferromagnetic (AFM) coupling between the magnetic layers in these multilayers. In many systems the AFM coupling exhibits oscillations in strength as a function of the thickness of the nonmagnetic layers separating the magnetic layers.[4-12] These oscillations are of fundamental physical interest because they often have a period much longer than would be expected on the basis of a free-electron Ruderman-Kittel-Kasuya-Yosida (RKKY) model. The coupling itself is of fundamental physical interest because of its often remarkably large strength.[4-12] As a result, the physical basis of these effects is presently the subject of intense theoretical investigation.[13]

These effects are also of great practical interest. The switching that produces the GMR effect consists of applying a magnetic field large enough to overcome the AFM coupling and thereby switching the multilayer from antiferromagnetic to ferromagnetic. At present, the fields required for this are too large to make the GMR effect practical as a basis for a new generation of electronic devices (such as nonvolatile dynamic random access memories), but if the AFM coupling could be made small, while maintaining a giant magnetoresistance, the technological impact would be profound.

The aim of the present work is to follow up earlier studies of the oscillations in AFM coupling in Fe/Cu/Fe multilayers grown on Cu(100) substrates,[12] with comparable studies of multilayers grown on a Cu(111) substrate, and thereby gain some insight into the crystallographic dependence of these effects. It is particularly noteworthy that while the earlier work using Cu(100) substrates found strongly oscillatory AFM coupling, the present work using a Cu(111) substrate finds no evidence of any such AFM coupling.

This result would seem to conflict with other studies of similar multilayers [reported to be (111) textured] grown by magnetron sputtering using Si-wafer substrates, which did show strongly oscillatory antiferromagnetic coupling.[5,7] A number of attempts were made in the present work [using molecular-beam-epitaxy (MBE) techniques] to mimic various aspects of the growth conditions occurring during magnetron sputtering; however, none produced any AFM coupling resembling that in Ref. 5 or 7. The most likely source of the apparent conflict in these observations would seem to be that, in the magnetron-grown multilayers, grains other than the (111)-oriented crystalline grains are responsible for the AFM coupling.

It is well known that in the textured film which are produced when metals are deposited on Si-wafer substrates, significant amounts of crystallographic orientations other than the textured (or dominant one) often occur.[14] Indeed, this is the reason for use of the term "textured", since the films are not single crystals of the type grown on single-crystal substrates by MBE techniques. Moreover, preliminary x-ray-diffraction pole-figure measurements we have made on three of the magnetron-grown multilayers (of Ref. 5) indicate that crystalline grains other than (111) are present.

The purpose of the present paper is to bring to the at-

tention of the research community the evidence suggesting that the AFM coupling found in the Fe/Cu/Fe and Co/Cu/Co multilayers grown by magnetron sputtering is not dominated by (111)-oriented crystalline grains. Instead, grains with other orientations, including those oriented at or near (100), apparently are responsible for the AFM coupling. This result suggests the possibility that the grains responsible for the AFM coupling may not be the ones responsible for the GMR.[15] Indeed, the contributions a grain makes to the AFM coupling and GMR might vary widely and differently, depending upon grain orientation. Consequently, it might be expected that fine tuning the distribution of grain orientations would be a way to achieve the much-sought-after goal of producing samples with giant magnetoresistance and small AFM coupling strength.

II. EXPERIMENT

The basic elements of the MBE system have been described in previous publications.[16–18] The Cu(111) single-crystal substrate was cut, oriented, and polished by procedures described in Ref. 19. The accuracy of the (111) alignment was $\pm 0.25°$.

The magneto-optical Kerr effect instrument used in this work to observe hysteresis loops was described in an earlier paper.[12] For the present work this instrument was modified so that both in-plane and polar Kerr measurements using a HeNe laser could be made *in situ* in the MBE system under ultrahigh-vacuum conditions. The absolute values of the polar Kerr rotation and ellipticity at 633 nm were calibrated with a quarter-wave plate, and the values in Tables I and II are accurate to better than $\pm 10\%$. The coercivities were determined using an *in situ* Hall probe, and the values reported are accurate to better than $\pm 10\%$. All samples were examined in fields up to 6 kOe, and some samples were taken to 7 kOe in the search for AFM coupling. The values reported in Tables I and II correspond to hysteresis loops measured at 80 K (300 K for sample 14 in Table II). Hysteresis loops were also recorded for these samples at many other temperatures in the search for AFM coupling, but except as discussed below, the values did not seem important enough to publish.

The measurement of in-plane hysteresis loops was sometimes made difficult by transient noise in the system. Whenever this problem was too severe for recording reliable loops, it was noted in the tables.

III. RESULTS AND DISCUSSION

Recent publications have demonstrated the existence of oscillatory AFM exchange coupling as a function of Cu spacer-layer thickness in Fe/Cu/Fe and Co/Cu/Co multilayers on Cu(100) substrates.[9,12] In related work similar exchange-coupling data have been obtained for Fe/Cu/Fe(100) structures where the entire structure is body-centered cubic (bcc).[6] Concurrently, oscillatory AFM coupling as function of Cu spacer-layer thickness has been observed in Fe/Cu/Fe and Co/Cu/Co multilayers [reportedly (111) textured] grown on Si-wafer substrates by magnetron sputtering.[5,7]

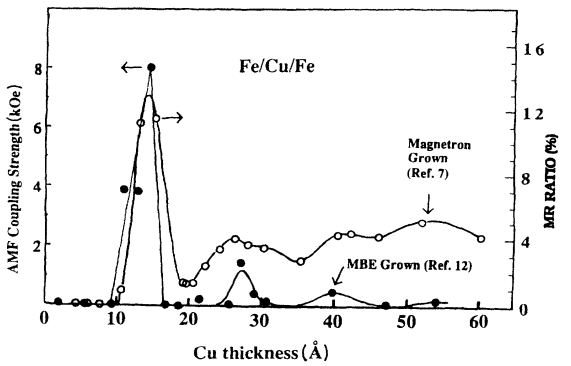

FIG. 1. Comparison of the oscillations in AFM-coupling strength for MBE-grown Fe/Cu/Fe multilayers on Cu(100) from Ref. 12 and the oscillations in the magnetoresistance ratio for magnetron-grown, (111)-textured Fe/Cu/Fe multilayers from Ref. 7.

A remarkable aspect of these results is that, although there are minor differences in detail among them, they are all generally consistent with the idea that the coupling in these films oscillates with a period of 12 ± 2 Å in spacer-layer thickness. The similarity is remarkable because, if the band structure of the Cu spacer layer is responsible for the effect, very different results might have been expected for Cu(100) and Cu(111) spacer-layer orientations.[13]

As a test of this expectation, a study of this coupling using a Cu(111) single-crystal substrate and MBE-growth methods [to achieve the highest possible degree of (111) crystalline perfection] would be very timely and of great interest. This was the motivation for the present study.

Figures 1 and 2 provide important background in the form of comparisons of data on MBE- and magnetron-grown Fe/Cu/Fe and Co/Cu/Co multilayers from the literature.[20] Although the figures compare different prop-

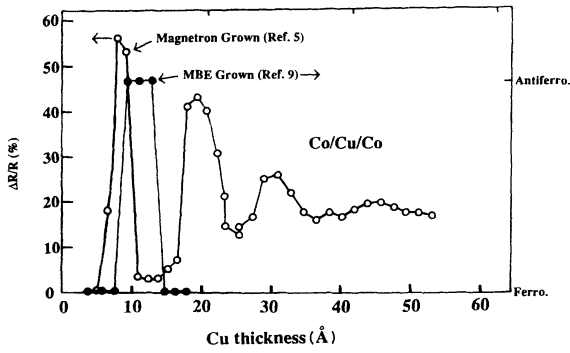

FIG. 2. Comparison of the oscillations in the magnetoresistance ratio for magnetron-grown, (111)-textured Co/Cu/Co multilayers from Ref. 5 and the oscillation in the AFM-FM coupling for MBE-grown Co/Cu/Co multilayers on Cu(100) from Ref. 9. Note that some flexibility may be called for in the comparison of thicknesses reported by groups using different growth conditions.

TABLE I. Summary of the Fe/Cu/Fe studies of this work, including the temperature of the substrate during deposition, the type of hysteresis loop observed [perpendicular ⊥ or in plane, ||], the coercivity, and the absolute values for the Kerr rotation Θ_K, and ellipticity ε_K. Note that these values could not be determined for in-plane samples. The annealing time was in each case ~20 s. For samples 17 and 20, the H_2 and CO pressures were 1×10^{-7} Torr and the *e*-beam flux was 2 μA/cm^2 at 15 keV. The Cu and Fe thicknesses are given in ML (to convert to Å, multiply by 2.085). In many cases below, lower annealing temperatures were also tried in the search for AFM coupling, but where little or no change was found, the results are not reported.

No.	Sample	Substrate temperature (K)	Loop type	H_c (Oe)	Θ_K	ε_K (10^{-3} deg)	
1	$Cu_5Fe_{2.8}Cu_{10}Fe_{3.0}$/Cu(111)	300	no loop				
2	$Cu_{4.5}Fe_{3.3}$/Cu(111)	300	no loop				
3	$Fe_{3.0}$/Cu(111)	300	no loop				
4	$Fe_{3.3}$/Cu(111)	80	⊥	120	3	22	
	300-K anneal		⊥	180		15	$T_c<300$ K
	450-K anneal		⊥	<10		4	
5	$Fe_{1.8}$/Cu(111)	80	⊥	<10		5	
6	$Fe_{4.6}$/Cu(111)	80	⊥	100	~0	32	
	300-K anneal		⊥	70	3.5	40	
	450-K anneal		⊥	65	3	41	
	550-K anneal		no loop				
7	$Cu_{4.8}Fe_{20.3}Cu_{10.0}Fe_{20.0}$/Cu(111)	80	||	10			
	500-K anneal		||	15			
	600-K anneal		||	15			
	750-K anneal		||	80			
	900-K anneal		no loop				
8	$Cu_{6.6}Fe_{20.5}Cu_{14.9}Fe_{20.2}$/Cu(111)	80	||	12			
	650-K anneal		||	12			
9	$Cu_{5.5}Fe_{21.6}Cu_{6.6}Fe_{21.5}$/Cu(111)	80	||	6			
	600-K anneal		||	8			
	825-K anneal		||	8			
	900-K anneal		||	16			
10	$Cu_{5.5}Fe_{21.0}Cu_{3.8}Fe_{20.9}$/Cu(111)	80	||	12			
	650-K anneal		||	14			
	750-K anneal		||	12			
11	$Cu_{4.8}Fe_{20.5}Cu_{5.9}Fe_{20.7}$/Cu(111)	80	||	8			
	750-K anneal		||	20			
12	$Cu_{5.1}Fe_{20.4}Cu_{5.3}Fe_{20.5}$/Cu(111)	300	||	15			
	750-K anneal		||	16			
13	$Cu_{6.3}Fe_{10.5}Cu_{6.7}Fe_{10.5}$/Cu(111)	300	||	25			
	700-K anneal		||	50			
14	$Cu_{6.0}Fe_{10.6}Cu_{8.8}Fe_{10.7}$/Cu(111)	300	||	32			
	700-K anneal		||	45			
15	$Cu_{4.8}Fe_{10.7}Cu_{12.6}Fe_{10.5}$/Cu(111)	300	||	45			
	700-K anneal		||	100			
16	$Cu_{6.0}Fe_{10.5}Cu_{6.7}Fe_{10.7}$/Cu(111)	300	||	80			(grown in H_2,CO)
	900-K anneal		||	1100			
17	$(Cu_7Fe_8)\times4$/Cu(111)	300	||	40			
	700-K anneal		||	160			

TABLE I. (*Continued*).

No.	Sample	Substrate temperature (K)	Loop type	H_c (Oe)	Θ_K	ε_K (10^{-3} deg)
18	$Fe_{7.6}Cu_{6.8}Fe_{8.4}/Cu(111)$	500	no loop			
19	$Cu_{6.0}Fe_{9.0}Cu_{6.7}Fe_{10.0}/Cu(111)$	300	||	50		(grown in H_2,Co, e^-)
20	$Cu_{5.2}Fe_{8.3}Cu_{2.9}Fe_{8.8}/Cu(111)$	300	||	80		

erties, this was all that was available. Nevertheless, there is general agreement that in these systems the oscillations in antiferromagnetic coupling are commensurate with oscillations in the magnetoresistance ratio.

In Fig. 1 it is noteworthy that the first and strongest peaks of the two data sets coincide in Cu thickness. The peaks at greater Cu thickness are also in good agreement. This is a remarkable result if the spacer layer responsible for it is Cu(100) in one case and Cu(111) in the other case. One hint that this may not be true is that in the MBE-grown Fe/Cu/Fe system the peak AFM coupling strength is 0.32 erg/cm^2 at 300 K.[12] In the magnetron-grown Fe/Cu/Fe multilayers, the coupling strength is reported to be 0.095 erg/cm^2 when measured at 4.2 K (it would be significantly smaller at room temperature).[7] Clearly, a minority component of ~(100)-oriented crystalline grains in the magnetron-grown multilayers could be responsible for, or at least contributing to, the AFM coupling observed in the magnetron-grown multilayers.

It is worth noting that single-crystal results for the Fe/Cu/Fe system give nearly the same Cu thickness for the first AFM maximum in both fcc and bcc growths.[6,12] The magnetron-grown multilayers of Ref. 7 were reported to contain a mixture of fcc Cu and bcc Cu in this thickness range.

Precise alignment of the minority component along (100) is probably not required to explain the data. In the extreme limit, it may even be the case that the tendency to (111) texture is small, that crystalline grains are almost random in alignment, and that only those grains within, say, ±20° of (100) contribute to the AFM coupling. Supporting this idea are preliminary x-ray-diffraction pole-figure measurements we have made on three of the samples of Ref. 5. The results clearly indicate the presence of crystalline grains other than (111). However, it is still possible that other orientations, in addition to the near-

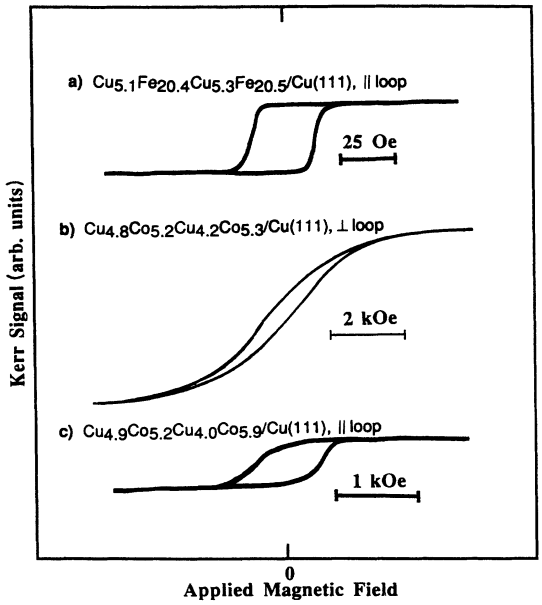

FIG. 3. Illustration of the Kerr ellipticity hysteresis loops for (a) the || loop of sample 12 of Table I as deposited, (b) the ⊥ loop for sample 5 of Table II as deposited, and (c) the || loop of sample 10 of Table II as deposited. For (c) a sloping background was substracted. Insets give the scale of the field for each loop. The Cu and Co thicknesses are given in ML (to convert to Å, multiply by 2.085).

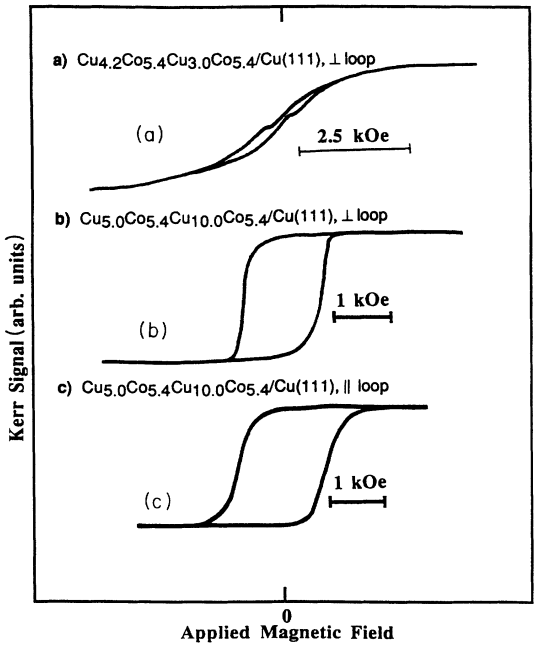

FIG. 4. Illustration of the Kerr ellipticity hysteresis loops for (a) the ⊥ loop of sample 6 of Table II after 700-K annealing, (b) the ⊥ loop for sample 13 of Table II as deposited, and (c) the || loop of sample 13 of Table II as deposited. For (c) a sloping background was substracted. Insets give the scale of the field for each loop. The Cu and Co thicknesses are given in ML (to convert to Å, multiply by 2.085).

TABLE II. Summary of the Co/Cu/Co studies of this work, including the temperature of the substrate during deposition, the type of hysteresis loop observed [perpendicular ($\perp$) or in plane ($\parallel$)], the coercivity, and the absolute values for the Kerr rotation Θ_K, and ellipticity ε_K. Note that these values could not be determined for in-plane samples. A^* means that the sample did not saturate in 6 kOe. A^{**} means that temporary noise in the instrument prevented that loop from being measured. The Cu and Co thicknesses are given in ML (to convert to Å, multiply by 2.085). In many cases below, lower annealing temperatures were also tried in the search for AFM coupling, but where little or no change was found, the results are not reported.

No.	Sample	Substrate temperature (K)	Loop type	H_c (Oe)	Θ_K	ε_K (10^{-3} deg)
1	$Co_{3.1}$/Cu(111)	300	$\perp$	no loop		
	same		$\parallel$	no loop		
2	$Co_{17.3}$/Cu(111)	300	$\perp$	110*		>100*
	same		$\parallel$	100		
3	$Cu_{5.3}Co_{18.3}Cu_{9.7}Co_{17.3}$/Cu(111)	300	$\perp$	~25*	~0	>100*
	same		$\parallel$	70		
4	$Cu_{4.5}Co_{5.4}Cu_{4.6}Co_{4.8}$/Cu(111)	80	$\perp$	340		82
	same		$\parallel$	no loop		
	700-K anneal		$\perp$	400	31	95
	same		$\parallel$	975		
	800-K anneal		$\perp$	170	(H_{AF}=100?)	207
	same		$\parallel$	**		
5	$Cu_{4.8}Co_{5.2}Cu_{4.2}Co_{5.3}$/Cu(111)	80	$\perp$	310	~0	177
	same		$\parallel$	no loop		
	700-K anneal		$\perp$	170	(H_{AF}=100?)	191
	same		$\parallel$	**		
6	$Cu_{4.2}Co_{5.4}Cu_{3.0}Co_{5.4}$/Cu(111)	80	$\perp$	400		176
	same		$\parallel$	50		
	700-K anneal		$\perp$	120	(H_{AF}=100?)	218
	same		$\parallel$	80		
7	$Cu_{6.7}Co_{5.2}$/Cu(111)	80	$\perp$	275		80
	same		$\parallel$	weak loop		
	700-K anneal		$\perp$	290		94
	same		$\parallel$	no data		
	$Cu_{4.4}Co_{5.0}$ added	80	$\perp$	625		110
	same		$\parallel$	175		
	700-K anneal		$\perp$	350		165
	same		$\parallel$	weak loop		
8	$Cu_{4.8}Co_{5.3}Cu_{6.6}Co_{5.5}$/Cu(111)	80	$\perp$	275		136
	same		$\parallel$	150		
	750-K anneal		$\perp$	550		195
	same		$\parallel$	750	(H_{AF}=650?)	
9	$Cu_{5.1}Co_{5.4}Cu_{6.7}Co_{5.6}$/Cu(111)	80–400	$\perp$	575		182
	same		$\parallel$	1050		
10	$Cu_{4.9}Co_{5.2}Cu_{4.0}Co_{5.9}$/Cu(111)	80–400	$\perp$	400	~0	99
	same		$\parallel$	400		
	500-K anneal		$\perp$	250		117
	same		$\parallel$	**		
	700-K anneal		$\perp$	250*		>125*
	same		$\parallel$	**		
11	$Cu_{4.9}Co_{5.3}Cu_{3.0}Co_{5.3}$/Cu(111)	80–400	$\perp$	475		73
	same		$\parallel$	no loop		
	700-K anneal		$\perp$	350		89
	same		$\parallel$	weak loop		

TABLE II. (*Continued*).

No.	Sample	Substrate temperature (K)	Loop type	H_c (Oe)	Θ_K	ε_K (10^{-3} deg)
12	$Cu_{5.5}Co_{5.3}Cu_{1.1}Co_{6.1}$/Cu(111)	80–400	⊥	225		154
	same		∥	550		
	700-K anneal		⊥	275		192
	same		∥	no data		
	900-K anneal		⊥	~25*		>140*
	same		∥	50		
13	$Cu_{5.0}Co_{5.4}Cu_{10.0}Co_{5.4}$/Cu(111)	80–400	⊥	675	82	150
	same		∥	800		
	700-K anneal		⊥	790		167
	same		∥	1375		
14	$Cu_{5.0}Co_{5.5}Cu_{4.1}Co_{5.3}$/Cu(111)	300	⊥	325	~0	110
	same		∥	205		

(100) orientations, contribute to the AFM coupling.

Figure 2 presents a similar comparison for Co/Cu/Co multilayers. It should be noted here that the data from Ref. 5, which used a Co thickness of 10 Å, is in near-perfect agreement with a corresponding data set in Ref. 7, which used a Co thickness of 15 Å. This suggests that the oscillations may be independent of Co thickness.

In Fig. 2 the agreement between MBE-and magnetron-grown multilayers is not as close as in Fig. 1. The first maximum in the two data sets differs by about 3 Å. However, it is interesting that both data sets in Fig. 2 suggest that the first maximum occurs for a smaller Cu thickness than is the case for Fe/Cu/Fe multilayers. It is also important to note that in systems such as these the segregation of Cu into a growing Co or Fe film can be a problem, particularly if the substrate is a little above room temperature.[16,21] This means that reported Cu spacer-layer thicknesses may be in error. Therefore some flexibility is called for in the comparison of thicknesses reported by groups using different growth conditions.

Tables I and II present a list of the Fe/Cu/Fe and Co/Cu/Co films we have investigated. None showed any evidence of AFM coupling as deposited. In order to extend the search for AFM coupling, many of these samples were subjected to brief annealing, as indicated in the tables. A few samples exhibited hysteresis loops that could be possible evidence of AFM coupling, but only after rather severe annealing (700–800 K) and without any systematic trends apparent. Certainly, there was no evidence of any coupling that in any way resembled the data of Refs. 5 and 7 (in which no annealing was required to observe AMF coupling).

Figures 3 and 4 present typical hysteresis loops observed for our samples.

A. Fe/Cu/Fe multilayers

In Table I samples 1–6 were preliminary experiments used to characterize the growth of Fe on Cu(111). This work included structural studies using low-energy electron diffraction (LEED) and x-ray photoelectron (XPS) forward scattering.[22] This work demonstrated that it is difficult to stabilize fcc Fe on Cu(111). Instead, a lattice very much like bcc Fe develops in the earliest stages of growth.

Annealing of these films was required to give a LEED pattern sharp enough for interpretation, but moderate annealing had remarkably little effect on the magnetic properties of the Fe, as can be seen in Table I. The LEED patterns exhibited spots, near the substate (1,0) spots, corresponding to the most intense reflections expected from the classic Nishiyama-Wassermann (NW) and Kurdjumov-Sachs (KS) epitaxial orientations at a [bcc (110)][fcc (111)] interface.[23,24] While this is consistent with the presence of both orientations, there were additional spots (corresponding to small reciprocal-lattice vectors), indicating that the structures were more complicated than simple NW and KS, probably involving a longer-range coincidence lattice between Fe and Cu. Samples 7–20 in Table I exhibited the same LEED pattern, with varying degrees of sharpness, depending on the preparation method.

Samples 8–11 were grown at cryogenic substrate temperature to suppress as effectively as possible any intermixing at the interfaces. The thicknesses were chosen to span the range in which antiferromagnetic coupling was found in the magnetron-grown samples. The hysteresis loops were generally found to be square and the coercivities low. Under these conditions a small step in the side of a loop (due to AFM coupling) could easily be detected at the 1-Oe level. None was seen, suggesting that if any AFM coupling exists, it must be at least three orders of magnitude smaller than that reported for the magnetron-grown samples.[7]

Samples 12–15 in Table I were deposited on the substrate at 300 K, which is closer to the conditions occurring in magnetron sputtering. Again, the loops were rather square, and no evidence of AFM coupling was found. In the search for AFM coupling, the samples were annealed to temperatures likely to promote bulk diffusion, but the induced changes were minor (the bulk heat of mixing of Fe and Cu is rather endothermic). Fig-

ure 3(a) illustrates the hysteresis loop for sample 12, as deposited.

Sample 16 was grown in 1.3×10^{-5} Pa (1×10^{-7} Torr) or H_2 and CO to mimic the reactive background gases likely to be present during magnetron sputtering. The motivation for this experiment was the well-established fact that adsorbed gases can sometimes modify epitaxial growth.[25] However, no AFM coupling was found, and indeed the effect of the gases on the magnetic properties was minor.

Sample 17 was grown to determine whether more than two Fe films are required for AFM coupling. The Cu spacer layer thickness of seven monolayers (ML) was chosen to correspond to the strongest AFM coupling in Ref. 7. However, none was found here.

Sample 18 was grown to determine the effect of using a substrate temperature high enough to make segregation of Cu into the growing Fe films significant (cf. Ref. 21). The motivation for this was the possibility that some heating of the substrates may occur in some magnetron-sputtering systems. However, this sample showed no hysteresis loop (using ±6 kOe), implying it was not ferromagnetic even at 80 K.

Sample 19 was grown as 16 was, but with the addition of irradiation by an electron gun defocused to cover the sample. The 15-keV beam spread a current of 2 μA over the 1-cm-diam sample. The motivation for this experiment was the fact that a magnetron gun acts as an electron flood gun, and there are reports of electron-beam-induced effects in AFM-coupled multilayers.[26] However, this sample showed no AFM coupling.

It would seem unlikely, in light of the work reported in Table I, that Cu(111) layers actually have some tendency to produce AFM coupling between Fe films. If any coupling on the order of the 1.4 kOe reported in Ref. 7 actually occurs, it should have been evident somewhere in the variety of samples studied here. If even a very small fraction of the sample volume of any of the samples studied here contained the Cu structure required for AFM coupling, it should have been apparent in the data.

Figure 5 presents a schematic illustration summarizing the model suggested here for the magnetron-grown multilayers. A variety of crystalline grains are present in the multilayer. The AFM coupling occurs through Cu grains oriented along or near the (100) axis. The magnetic moment in the Fe grains couples ferromagnetically across the grain boundaries. In this way the grains within each Fe film are ferromagnetically aligned, but aligned antiferromagnetically across the Cu for two adjacent Fe films.

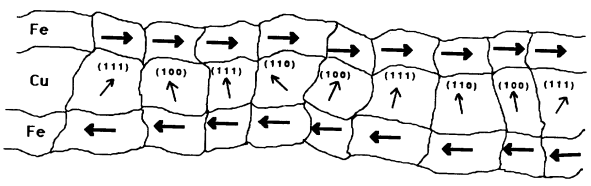

FIG. 5. Schematic illustration of the model suggested here for the grain and magnetic structures of magnetron-grown multilayers. The bold arrows in the Fe region represent the magnetic moment, and the light arrows in the Cu region represent the indicated crystallographic orientation of the grain.

B. Co/Cu/Co multilayers

Table II presents data on the Co/Cu/Co multilayers. It was found in preliminary structural studies that the structure of epitaxial Co films on Cu(111) is particularly simple. In the range of thicknesses studied here, epitaxial Co films grow as fcc Co with occasional stacking faults which cause the symmetry of the LEED pattern to transform gradually, from threefold to sixfold, during the growth of the multilayer. The LEED pattern is strictly 1×1, and only the films grown at cryogenic temperatures and not subjected to annealing exhibited strongly broadened LEED spots. The stacking faults seem to be an intrinsic feature of growth at 300 K or below in this system, and their presence should thus be expected in magnetron-grown multilayers. It may be that these stacking faults play some important role in the behavior of these multilayers.

Even if no stacking faults occur during the growth of the Cu spacer layers themselves, the fact that the underlying Co film contains grown-in stacking faults means that grain boundaries will be present in the Cu. It is noteworthy that stacking faults generally do not occur in growth of Fe or Co on Cu(100) surfaces,[17,21] and so in these systems the spacer layers should not be defective.

For samples 4–14 the Co thickness was chosen to be ~5 ML (10 Å) to match the results in Ref. 5 for magnetron-grown Co/Cu/Co multilayers. However, as discussed above, the near-perfect agreement between the data sets of Refs. 5 and 7 suggests that the Co thickness is not very important.

The T_c values for these samples, as deposited, were difficult to estimate because temperatures high enough to shrink the loop resulted both in irreversible changes in the loop after cooling down and in sharpening of the LEED spots.

The in-plane hysteresis loops for the Co multilayers were generally somewhat square, while the perpendicular loops were generally strongly skewed or S shaped with a remanance that was often only 10–20% of saturation. The perpendicular loops often required 2–5 kOe to achieve saturation. Figures 3(b) and 3(c) illustrate typical results.

Furthermore, for samples 6–8, the in-plane coercivity, for as-deposited films, was much smaller than the perpendicular coercivity, suggesting that the moment in these samples is very likely canted so as to be almost in plane. (This canting would require a larger perpendicular field to switch the moment because of the torque being reduced by $\cos\Theta$, where Θ is the angle between the applied field and moment.) The use here of the term "coercivity" assumes that switching occurs by domain-wall motion. If coherent rotation were the mechanism, then the values reported would be a mixture of coercivity and anisotropy field. This canting seems to be affected by the film-growth procedures, which is not surprising since anisot-

ropy is well known to be very structure sensitive. Samples 9–13, which were grown by methods which produce the sharpest interfaces possible, exhibited coercivities that suggest the anisotropy was still canted, but closer to perpendicular than in samples 6–8.

Samples 4–8 were grown at cryogenic substrate temperatures to suppress as effectively as possible any intermixing at the interfaces. After deposition the LEED spots were rather fuzzy, appearing visually to be perhaps 10% of a reciprocal-lattice vector wide. Annealing to 700 K reduced this width by perhaps a factor of 4. The thicknesses of this set of samples were chosen to span the range where antiferromagnetic coupling was found in the magnetron-grown samples.[5,7]

No evidence of AFM coupling was found in any of these samples as deposited. However, three samples, 4,5, and 6, exhibited weak steps in their perpendicular loops which could be attributed to AFM coupling of ~ 100 Oe after annealing to 700–800 K. However, this effect was only observed when these samples were held at 150–250 K. Figure 4(a), recorded at 200 K, illustrates this effect. Outside this temperature range, the sides of the loops were smooth. This observation of such a fleeting effect, after such severe annealing (likely to produce bulk diffusion), would not seem adequate to explain so robust an effect as was found in the magnetron-grown samples.

Another possible case of AFM coupling was found in sample 8, but only after annealing to 750 K. The in-plane loop had the classic stair-step appearance of a sample in which the coercivity and AFM coupling are of similar magnitude. An alternative interpretation would be that the Co films couple ferromagnetically, but have different coercivities (100 and 1300 Oe). If so, the heights of the stair steps would then imply that the deeper Co film had the smaller coercivity, as if the annealing mainly affected the top Co film (annealing generally increases coercivity in this system). However, the loop was strong only below 100 K and shrank to nothing by 300 K. Moreover, the spacer-layer thickness of 6.6 ML (14 Å) is not where the magnetron-grown samples showed AFM coupling,[5,7] and no other sample in this study exhibited such behavior. Thus this result seems to be an anomaly, with no bearing on the AFM coupling which occurs in the magnetron-grown multilayers.

Since the size of the LEED spots for samples 4–8 indicated that, as deposited, they contained numerous defects, a procedure was developed paralleling the work of Refs. 12 and 16 to achieve atomically sharp interfaces and the best crystalline order. The procedure involved depositing the Co at a substrate temperature of 80–100 K, annealing the Co to 400 K after deposition, depositing the Cu at 350 K, then cooling the substrate again for the next Co deposition, etc. This growth technique suppresses the well-known tendency of Cu to segregate during Co deposition.[16,21] It also yields very sharp LEED spots which imply in-plane order of longer range than the thickness of the multilayer. Thus each grain of the multilayer can be described as a nearly perfect single-crystalline unit.

Samples 9–13 were grown by this improved technique. None showed any evidence of AFM coupling. The in-plane hysteresis loops were approximately square, and the perpendicular loops were skewed (except for sample 13, which had almost 100% remanance). Of particular note are samples 10 and 13, which had Cu spacer-layer thicknesses equal to the first two maxima of the AFM coupling of the magnetron-grown samples.[5,7] Figures 4(b) and 4(c) illustrate the loops for sample 13, as deposited.

Sample 14 was grown entirely at 300 K and had nearly as good a LEED pattern as its analog, sample 10. However, no evidence of AFM coupling was found. The perpendicular loop was skewed and the in-plane loop square, as before.

The above results taken all together make it seem unlikely that even highly crystalline Cu(111) layers provide AFM coupling between Co films. Pinholes in the Cu spacer layers (to act as a ferromagnetic bridge between Co films) cannot be ruled out completely, but we consider such an explaination to be very unlikely. Low substrate temperatures during deposition should suppress diffusion and thus pinholes. Moreover, our earlier work on Cu(100) using similar growth techniques found AFM coupling,[12] so pinholes evidently were not a problem. In any case, if pinholes were a problem here, they should also have been a problem in the magnetron-grown multilayers.

It may be of interest to note in passing that the magneto-optical activity of most of these samples is considerably enhanced over that expected on the basis of the bulk optical constants of Co. This enhancement is similar to that reported for Fe/Cu/Fe multilayers in Ref. 12. For example, sample 13 (the only multilayer in Table II that exhibited, as deposited, a nearly square perpendicular loop) has a maximum Kerr rotation $(\Theta_K^2+\varepsilon_K^2)^{1/2}$ of 0.170°, which is surprisingly large given its total content of only 10.8 ML of Co. The bulk optical constants for Co and Cu for left and right circularly polarized light predict a value of 0.080° for this structure.

IV. CONCLUSIONS

The major points of this work can be summarized as follows.

(1) No consistent evidence of antiferromagnetic coupling is observed for MBE-grown Fe/Cu/Fe and Co/Cu/Co multilayers on Cu(111) substrates.

(2) In contrast, oscillatory antiferromagnetic coupling *is* observed for Fe/Cu/Fe and Co/Cu/Co multilayers reportedly exhibiting (111) texture and grown on Si-wafer substrates by magnetron sputtering.[5,7]

(3) The above points (1) and (2) seem to present a conflict. However, oscillatory antiferromagnetic coupling *has* been observed for MBE-grown Fe/Cu/Fe (Ref. 12) and Co/Cu/Co (Ref. 9) multilayers on Cu(100) substrates.

(4) Preliminary x-ray-diffraction pole-figure data on several of the magnetron-grown multilayers indicate that the (111) texture is weak, meaning that crystalline grains other than (111) are present. Furthermore, the oscillations in the (111)-textured, magnetron-grown samples and (100) MBE-grown samples are similar, and the agreement

is within the uncertainty of the film-thickness determinations.

(5) Point (4) suggests that a minority constituent of ~(100)-oriented crystalline grains present in the magnetron-grown multilayers could be partly, or perhaps even largely, responsible for the observed antiferromagnetic coupling.

(6) There could also be grains of other orientation contributing to the antiferromagnetic coupling observed in the magnetron-grown samples, but surprisingly, (111)-oriented grains are apparently not contributing.

(7) If this interpretation is correct, many crystalline grains are likely to be contributing to the giant magnetoresistance effect, so that reducing the concentration of those crystalline grains responsible for the antiferromagnetic coupling in the multilayer [such as (100)] should be a way to lower the antiferromagnetic coupling strength while maintaining the giant magnetoresistance effect.

ACKNOWLEDGMENTS

The authors gratefully acknowledge very helpful conversations with Dr. R. Coehoorn, Dr. P. M. Levy, Dr. R. F. C. Farrow, Dr. B. Heinrich, Dr. S. S. P. Parkin, and Dr. F. Herman. We wish to thank Dr. R. F. C. Farrow and Dr. S. S. P. Parkin for loaning us several of their Co/Cu/Co multilayer samples for x-ray-diffraction pole-figure analysis. This work was supported, in part, by the Office of Naval Research, Contract No. N00014-91-F-0044.

[1]M. N. Baibich, J. Broto, A. Fert, F. Nguyen Van Dau, F. Petroff, P. Eitenne, G. Creuzet, A. Friederich, and J. Chazelas, Phys. Rev. Lett. **61**, 2472 (1988); P. Etienne, G. Creuzet, A. Friederich, F. Nguyen-Van-Dau, and A. Fert, Appl. Phys. Lett. **53**, 162 (1988); P. Etienne, J. Chazelas, G. Creuzet, A. Friederich, J. Massies, F. Nguyen-Van-Dau, and A. Fert, J. Cryst. Growth **95**, 410 (1989).

[2]G. Binasch, P. Grünberg, F. Sauernbach, and W. Zinn, Phys. Rev. B **39**, 4828 (1989); F. Saurenbach, J. Barnas, G. Binasch, M. Vohl, P. Grünberg, and W. Zinn, Thin Solid Films **175**, 317 (1989).

[3]E. Vélu, C. Dupas, D. Renard, J. P. Renard, and J. Seiden, Phys. Rev. B **37**, 668 (1988).

[4]S. S. P. Parkin, N. More, and K. P. Roche, Phys. Rev. Lett. **64**, 2304 (1990); S. S. P. Parkin, *ibid.* **67**, 3598 (1991).

[5]S. P. P. Parkin, R. Bahdra, and K. P. Roche, Phys. Rev. Lett. **66**, 2152 (1991); S. S. P. Parkin, Z. G. Li, and K. J. Smith, Appl. Phys. Lett. **58**, 2710 (1991); S. S. P. Parkin, Phys. Rev. Lett. **67**, 3598 (1991); S. S. P. Parkin and D. Mauri, Phys. Rev. B **44**, 7131 (1991).

[6]B. Heinrich, Z. Celinski, J. F. Cochran, W. B. Muir, J. Rudd, Q. M. Zhong, A. S. Arrott, K. Myrtle, and J. Kirschner, Phys. Rev. Lett. **64**, 673 (1990).

[7]D. H. Mosca, F. Petroff, A. Fert, P. A. Schroeder, W. P. Pratt, Jr., and R. Laloee, J. Magn. Magn. Mater. **94**, L1 (1991); F. Petroff, A. Barthélémy, D. H. Mosca, D. K. Lottis, A. Fert, P. A. Schroder, W. P. Pratt, Jr., and R. Loloee, Phys. Rev. B **44**, 5355 (1991); A. Fert, A. Barthélémy, P. Etienne, S. Lequien, R. Loloee, D. H. Mosca, F. Petroff, W. P. Pratt, Jr., and P. A. Schroder (unpublished).

[8]Z. Celinski and B. Heinrich, J. Magn. Magn. Mater. **99**, L25 (1991); B. Heinrich, Z. Celinski, K. Myrtle, J. F. Cochran, M. Kowalewski, A. S. Arrott, and J. Kirschner, J. Appl. Phys. (to be published); J. Magn. Magn. Mater. (to be published).

[9]J. J. de Miguel, A. Cebollada, J. M. Gallego, R. Miranda, C. M. Schneider, P. Schuster, and J. Kirschner, J. Magn. Magn. Mater. **93**, 1 (1991); A. Cebollada, R. Miranda, C. M. Schneider, P. Schuster, and J. Kirschner, *ibid.* **102**, 1 (1991); J. J. de Miguel, A. Cebollada, J. M. Gallego, and R. Miranda (unpublished).

[10]J. J. Krebs, P. Lubitz, A. Chaiken, and G. A. Prinz, Phys. Rev. Lett. **63**, 1645 (1989); N. Hosoito, S. Araki, K. Mibu, and T. Shinjo, J. Phys. Soc. Jpn. **59**, 1925 (1990); W. Vavra, C. H. Lee, F. J. Lamelas, H. R. Clarke, and C. Uher, Phys. Rev. B **42**, 4889 (1990); M. E. Burbaker, J. E. Mattson, C. H. Sowers, and S. D. Bader, Appl. Phys. Lett. **58**, 2306 (1991); P. Grünberg, S. Democritov, A. Fuss, M. Vohl, and A. Wolf, J. Appl. Phys. **69**, 4789 (1991); P. Grünberg, J. Barnas, F. Saurenbach, A. Fuss, A. Wolf, and M. Vohl, J. Magn. Magn. Mater. **93**, 58 (1991); J. Unguris, R. J. Celotta, and D. T. Pierce, Phys. Rev. Lett. **76**, 140 (1991); S. T. Purcell, W. Folkerts, M. T. Johnson, M. W. E. McGee, K. Jager, J. aan de Stegge, W. B. Zeper, W. Hoving, and P. Grünberg, *ibid.* **67**, 903 (1991); W. Chen, M. Onellion, and A. Wall (unpublished); H. Yamamoto, T. Okuyama, H. Dohnomae, and T. Shinjo (unpublished); Y. Y. Huang, G. P. Felcher, and S. S. P. Parkin, J. Magn. Magn. Mater. **99**, L31 (1991).

[11]B. Dieny, V. S. Speriosu, B. A. Gurney, S. S. P Parkin, D. R. Wilhoit, K. P. Roche, S. Metin, D. T. Peterson, and S. Nadimi, J. Magn. Magn. Mater. **93**, 101 (1991); B. Dieny, V. S. Speriosu, S. S. P. Parkin, B. A. Gurney, D. R. Wilhoit, and D. Mauri, Phys. Rev. B **43**, 1297 (1991); B. Dieny, V. S. Speriosu, and S. Metin, Europhys. Lett. (to be published); B. Dieny, P. Humbert, V. S. Speriosu, S. Metin, B. A. Gurney, P. Baumgart, and H. Lefakis (unpublished).

[12]W. R. Bennett, W. Schwarzacher, and W. F. Egelhoff, Jr., Phys. Rev. Lett. **65**, 3169 (1990).

[13]R. E. Camley and J. Barnas, Phys. Rev. Lett. **63**, 664 (1989); P. M. Levy, S. Zhang, and A. Fert, *ibid.* **65**, 1643 (1990); F. Trigui, E. Velu, and C. Dupas, J. Magn. Magn. Mater. **93**, 421 (1991); W. Schmidt, *ibid.* **93**, 418 (1991); C. Lacroix and J. P. Gavigan, *ibid.* **93**, 413 (1991); D. Stoeffler, K. Ounadjela, and F. Gautier, *ibid.* **93**, 386 (1991); W. Folkerts, *ibid.* **93**, 302 (1991); D. W. Edwards and J. Mathon, J. *ibid.* **93**, 85 (1991); P. M. Levy and S. Zhang, *ibid.* **93**, 67 (1991); A. Barthelemy and A. Fert, Phys. Rev. B **43**, 13 124 (1991); Y. Wang, P. M. Levy, and J. L. Fry, Phys. Rev. Lett. **65**, 2732 (1990); J. L. Fry, E. C. Ethridge, P. M. Levy, and Y. Wang, J. Appl. Phys. **69**, 4780 (1991); C. Chappert and J. P. Renard, Europhys. Lett. **125**, 553 (1991); D. M. Edwards, J. Mathon, R. B. Muniz, and M. S. Phan, J. Magn. Magn. Mater. **93**, 85 (1991); J. Phys. Condens. Mater **3**, 4941 (1991); Phys. Rev. Lett. **67**, 493 (1991); P. Bruno and C. Chappert, *ibid.* **67**, 1602 (1991); R. Coehoorn, Phys. Rev. B **44**, 9331 (1991); B. L. Johnson and R. E. Camley, *ibid.* **44**, 9997 (1991); M. Johnson, Phys. Rev. Lett. **67**, 3594 (1991); F. Herman, J. Sticht, and M. Van Schilfgaarde, Proc. Mater. Res. Soc. **231**, 195 (1992).

[14]H. Sato, P. A. Schroder, J. Slaughter, W. P. Pratt, Jr., and W. Abdul-Razzag, Superlatt. Microstruct. **4**, 45 (1987); D. H. Mosca, A. Barthelemy, F. Petroff, A. Fert, P. A. Schroeder,

W. P. Pratt, Jr., R. Laloee, and R. Cabanel, J. Magn. Magn. Mater. **93**, 480 (1991); C.-A. Chang, *ibid.* **96**, L7 (1991).

[15]This concept is consistent with the work of Ref. 11, which showed that exchange-biased CoCu multilayers can exhibit a large magnetoresistance without oscillatory AFM coupling.

[16]D. A. Steigerwald, I. Jacob, and W. F. Egelhoff, Jr., Surf. Sci. **202**, 472 (1988).

[17]D. A. Steigerwald and W. F. Egelhoff, Jr., J. Vac. Sci. Technol. A **7**, 3123 (1989).

[18]W. F. Egelhoff, Jr., I. Jacob, J. M. Rudd, J. F. Cochran, and B. Heinrich, J. Vac. Sci. Technol. A **8**, 1582 (1990).

[19]J. F. Cochran, W. B. Muir, J. M. Rudd, B. Heinrich, Z. Celinski, T. T. LeTran, W. Schwarzacher, W. R. Bennett, and W. F. Egelhoff, Jr., J. Appl. Phys. **69**, 5206 (1991).

[20]The comparisons in Figs. 1 and 2 are made in terms of Cu thickness in Å, which is the natural unit of measure since all groups use quartz-crystal-oscillator thin-film thickness monitors. In this way the same number of Cu atoms deposited per unit surface area by the different groups is being compared. A comparison in terms of Cu monolayers would be misleading unless the crystalline orientation of growth were known and were the same in the different experiments, since different crystal planes have different spacings.

[21]G. J. Mankey, M. T. Kief, and R. F. Willis, J. Vac. Sci. Technol. A **9**, 1595 (1991).

[22]For a review of XPS forward scattering, see W. F. Egelhoff, Jr., CRC Crit. Rev. Solid State Mater. Sci. **16**, 213 (1990).

[23]H. L. Gaigher and N. G. van der Berg, Thin Solid Films **196**, 111 (1991).

[24]For a good review, see E. Bauer and J. H. van der Mewre, Phys. Rev. B **33**, 3657 (1986).

[25]W. F. Egelhoff, Jr., J. Vac. Sci. Technol. A **7**, 2167 (1989).

[26]S. Demokritov (private communication).